

**Methodology for  
prediction of risk**

A. Baklanov et al.

# Methodology for prediction and estimation of consequences of possible atmospheric releases of hazardous matter: “Kursk” submarine study

A. Baklanov<sup>1</sup>, A. Mahura<sup>1,2</sup>, and J. H. Sørensen<sup>1</sup>

<sup>1</sup>Danish Meteorological Institute, 2100 Copenhagen, Denmark

<sup>2</sup>Kola Science Centre, Apatity, 184200, Russia

Received: 12 November 2002 – Accepted: 24 February 2003 – Published: 17 March 2003

Correspondence to: A. Baklanov (alb@dmi.dk)

Title Page

Abstract

Introduction

Conclusions

References

Tables

Figures

◀

▶

◀

▶

Back

Close

Full Screen / Esc

Print Version

Interactive Discussion

© EGU 2003

## Abstract

There are objects with some periods of higher than normal levels of risk of accidental atmospheric releases (nuclear, chemical, biological, etc.). Such accidents or events may occur due to natural hazards, human errors, terror acts, and during transportation of waste or various operations at high risk. A methodology for risk assessment is suggested and it includes two approaches: 1) probabilistic analysis of possible atmospheric transport patterns using long-term trajectory and dispersion modelling, and 2) forecast and evaluation of possible contamination and consequences for the environment and population using operational dispersion modelling. The first approach could be applied during the preparation stage, and the second – during the operation stage. The suggested methodology is applied on an example of the most important phases (lifting, transportation, and decommissioning) of the “Kursk” nuclear submarine operation.

It is found that the temporal variability of several probabilistic indicators (fast transport probability fields, maximum reaching distance, maximum possible impact zone, and average integral concentration of  $^{137}\text{Cs}$ ) showed that the fall of 2001 was the most appropriate time for the beginning of the operation. These indicators allowed to identify the hypothetically impacted geographical regions and territories. In cases of atmospheric transport toward the most populated areas, the forecasts of possible consequences during phases of the high and medium potential risk levels based on a unit hypothetical release are performed. The analysis showed that the possible deposition fractions of  $10^{-11}$  over the Kola Peninsula, and  $10^{-12} - 10^{-13}$  for the remote areas of the Scandinavia and Northwest Russia could be observed.

The suggested methodology may be used successfully for any potentially dangerous object involving risk of atmospheric release of hazardous materials of nuclear, chemical or biological nature.

## Methodology for prediction of risk

A. Baklanov et al.

Title Page

Abstract

Introduction

Conclusions

References

Tables

Figures

◀

▶

◀

▶

Back

Close

Full Screen / Esc

Print Version

Interactive Discussion

## 1. Introduction

There are some risk objects with higher than usually level of risk of accidental atmospheric releases (nuclear, chemical or biological) during limited time periods of special actions. Such accidents may occur during transportation of waste, or may be due to natural hazards, human errors, terror acts etc. and various operations at high risk.

On 12 August 2000, the “Kursk” nuclear submarine (KNS) after an accident during exercises of the Russian Northern Fleet (RNF) sunk with its 118 crew members in the aquatoria of the Barents Sea (69.62° N and 37.57° E, cf. Fig. 1). A presumed cause of the accident is the blast of a torpedo (Findings, 2002). The successful complex operation of the nuclear submarine (NS) lifting and transportation took place in fall 2001, following the preparation stage. The submarine was lifted on 8 October 2001, and then transported through the Kola Bay to a dry dock of the Roslyakovo shipyard (69.08° N and 33.17° E, Murmansk region, Russia) on 21 October 2001 (cf. Fig. 1). After the necessary preparations the “Granit” cruise missiles (in total 16) were removed from the submarine. Then in April 2002, the submarine was moved into the floating dock “Pallada” and was transported in the dock of the repairing shipyard “Nerpa” in the Snezhnogorsk town (69.33° N and 32.83° E, cf. Fig. 1).

According to the RNF plans (ITAR-TASS, 2002) the removal of a nuclear reactor from KNS and scrapping of its hull will be finished during October–November 2002. The remaining 6 damaged missiles were removed from the submarine in late July 2002. Some of these missiles will be transported to a storage base and some (which cannot be removed) will be blasted in the Barents Sea in an area located 58 kilometres from Severomorsk (the RNF headquarters) or in an open pit of the Lovozero area (the blasting place – 68.9° N and 34.7° E, cf. Fig. 1). “The blasting of the missiles does not make any ecological danger, as there is no fuel in them anymore and only explosive remained,” the navy officials said (Kursk-web-side, 2002). The KNS hull will be cut into three parts. The nuclear reactor will be removed from the central portion. Some fragments of the KNS nose compartment had been recovered from the Barents Sea floor

### Methodology for prediction of risk

A. Baklanov et al.

Title Page

Abstract

Introduction

Conclusions

References

Tables

Figures

◀

▶

◀

▶

Back

Close

Full Screen / Esc

Print Version

Interactive Discussion

**Methodology for prediction of risk**

A. Baklanov et al.

Title Page

Abstract

Introduction

Conclusions

References

Tables

Figures

◀

▶

◀

▶

Back

Close

Full Screen / Esc

Print Version

Interactive Discussion

© EGU 2003

and transported to St. Petersburg. Thus, the KNS operation involved several phases with different potential risk levels including: (i) lifting in the Barents Sea and transportation through the Kola Bay to the shipyard in Roslyakovo; (ii) setting on the dry dock and removal of the undamaged missiles; (iii) transportation to the “Nerpa” shipyard in Snezhnogorsk; (iv) removal of the damaged missiles; (v) removal of the nuclear reactors and scrapping of the submarine; (vi) lifting of the first compartment parts and blasting of the remaining parts. Following the potential risk categories, suggested by Bergman and Baklanov (1998), a very rough potential risk level ranging for the KNS operation phases is shown in Table 1.

News media including Internet web-sites (e.g. see Kursk-web-site, 2001–2002) provided information about activities and tasks, steps of the operation as well as meteorological conditions in the region. It should be noted that several organisations, including RNF, took part in the preparation and performance of this operation. The measurements of the radioactivity near the sunken submarine in the Barents Sea were carried out by the Murmansk Marine Biological Institute, Kola Science Centre (Matishov et al., 2002). It showed that the radioactivity level around the submarine was insignificantly increased, but it was very similar to the background radiation level in the Barents Sea. The water spread of possible radioactive substances from KNS in the Barents and other Arctic seas was predicted by the German scientists (Gerdes et al., 2001). The normative documents on the safety conditions and emergency preparedness for the lifting phase of the KNS operation were carefully elaborated by official experts of several ministries of the Russian Federation (Lifting, 2001). However, a general analysis of atmospheric transport and possible consequence forecast were not realised, only a simple risk assessment for the local scale was performed.

Hence, it was very important, from one side, to carry out a risk assessment before the phases started, as well as from other side, to forecast and evaluate the possible airborne contamination and consequences using operational dispersion modelling during the high and medium risk phases of the KNS operation (Table 1). It became more or less clear now that the risk of a severe accident with a large atmospheric release

was quite low, but at the moment of the accident and during stages of the operational forecasting such analysis of possible risk and reactor conditions were not available. Therefore, in such cases researchers considered the worst-case hypothetical accident scenarios, geophysical conditions, meteorological situations, and most dangerous possible situations.

## 2. Methodology

In this study, a method for the risk assessment including two approaches – for the preparation and for the operation stages – in order to evaluate possible atmospheric transport, contamination, and consequences as a result of hypothetical accidental releases at any of the nuclear risk sites (NRSs) is suggested. The Kursk nuclear submarine was selected as an example of such a risk site. In Mahura et al. (2003) the method with a brief discussion was applied for the phases of the lifting preparation and KNS lifting during September–October 2001. After that, during 2001–2002, the KNS operation had continued and followed several phases/actions as shown in Table 1. During this time the geographical location of the submarine had changed several times: starting from the accident location in the Barents Sea and ending in the “Nerpa” shipyard of the Snezhnogorsk town on the Kola Peninsula (Fig. 1).

A reviewer of the paper by Mahura et al. (2003) stressed the importance of the evaluation of dispersion and deposition modelling patterns, the estimation of possible radioactive concentrations in the environment, and exposure doses from potential releases of radioactive substances from KNS. Therefore, in this paper, more detailed description of the suggested method and its extended demonstration with a focus on the assessment of the possible risk and atmospheric transport of hypothetical releases are considered for several phases of the operation – the lifting, transportation, and decommissioning steps in Roslyakovo and Snezhnogorsk.

The first approach in this method is the probabilistic analysis of possible atmospheric transport and deposition/concentration patterns from the site using trajectory or/and

### Methodology for prediction of risk

A. Baklanov et al.

Title Page

Abstract

Introduction

Conclusions

References

Tables

Figures

◀

▶

◀

▶

Back

Close

Full Screen / Esc

Print Version

Interactive Discussion

dispersion modelling. This approach can be used during the preparation stage, i.e. when there are initial steps requiring consideration of the goals, tasks, temporal and spatial frames, etc.

The second approach consists of evaluation of the possible contamination and consequences using real-time operational dispersion modelling. This approach could be used in the late phase of the preparation stage as well as during different phases of the operation stage, i.e. when there are particular measures taken to perform an operation (for example, lifting or transportation of the damaged object posing a risk, decontamination of the polluted area and/or facility, etc.). It should be stressed that although the sunken nuclear submarine was selected as an example for this study, it might have been any object of potential nuclear, chemical or biological danger.

## 2.1. Approach for preparation stage

At the preparation stage, an approach, which includes three research tools, is suggested. These tools are the following: 1) isentropic trajectory modelling (ITM), 2) dispersion and deposition modelling (DDM), and 3) set of statistical analysis procedures, including probability fields analysis (PFA), to explore the structure of the calculated trajectory datasets. The isentropic trajectory model (based on a technique by Merrill et al., 1985) was used to calculate isentropic forward trajectories originated over the sunken NS location during 1987–1996. The dispersion and deposition model DERMA (Sørensen, 1998; Sørensen et al., 1998; Baklanov and Sørensen, 2001) was used to calculate the concentration and deposition fields due to hypothetical accidental releases of radioactivity from different geographical locations during the KNS operation. The probability fields analysis (Mahura et al., 2001; Mahura and Baklanov, 2002) was used to construct the monthly and seasonal fast transport probability fields, maximum reaching distance and maximum possible impact zone indicators representing atmospheric transport patterns during the first day of transport from the sites in order to identify the most impacted geographical regions and territories.

## Methodology for prediction of risk

A. Baklanov et al.

Title Page

Abstract

Introduction

Conclusions

References

Tables

Figures

◀

▶

◀

▶

Back

Close

Full Screen / Esc

Print Version

Interactive Discussion

### 2.1.1. Trajectory modelling

The trajectory modelling is a useful tool to evaluate common airflow patterns within meteorological systems on various scales. In this study, among different approaches to model atmospheric trajectories, the isentropic approach was selected. Although trajectory models based on such assumption (adiabatically moving air parcels) and neglect by various physical effects, they are still a useful tool if the long-period statistics is needed and computational resources is a critical issue. There are, of course, some uncertainties in these models too, and they are related to the meteorological data interpolation, assumptions of vertical transport, etc. (Stohl, 1998).

In this study, the National Center for Environmental Prediction (NCEP, USA) original gridded wind fields from the DS-082.0 dataset (“NCEP Global Tropospheric Analyses”) of the National Center for Atmospheric Research (NCAR, Boulder, Colorado, USA) were interpolated to potential temperature (isentropic) surfaces. The interpolated wind fields then were used to calculate forward isentropic trajectories in the model domain (20° N–85° N vs. 60° W–127.5° E) for two NRSs: 1) the sunken NS (over the surface of the Barents Sea) and 2) Kola nuclear power plant (over the land surface in the central part of the Kola Peninsula). Due to the fact that during operation the geographical location of the Kursk NS had changed (site of accident in the Barents Sea, water path of the NS transportation, shipyards in Roslyakovo and Snezhnogorsk), it was important to consider the possibility of changes in the atmospheric transport patterns for the water and land locations.

The trajectories originating over the Kola nuclear power plant (NPP) region were used from a study by Mahura et al. (2001). For the KNS region, the trajectories were calculated for a period of 10 years (1987–1996) twice per day (at 00:00 and 12:00 UTC, Universal Co-ordinated Time) at various levels (in total 16) within the atmosphere. From all calculated trajectories (more than 467 thousands) only those having origin near the surface (more than 29 thousands) were selected for the further statistical analysis.

## Methodology for prediction of risk

A. Baklanov et al.

Title Page

Abstract

Introduction

Conclusions

References

Tables

Figures

◀

▶

◀

▶

Back

Close

Full Screen / Esc

Print Version

Interactive Discussion

## 2.1.2. Dispersion modelling

The trajectory modelling does not consider one of the important mechanisms of the airborne contamination – the removing processes, e.g. the wet deposition, which is most important for the deposition fields. The dispersion modelling can resolve this gap.

The DERMA model (see Sect. 2.2) with the DMI-HIRLAM meteorological analyzed archived fields was used for the long-term dispersion simulation with a permanent or periodical discrete release at a NRS. The simulation period considered is October 2001 – October 2002. Several characteristics were calculated for the released radionuclide <sup>137</sup>Cs: 1) surface air concentration of radionuclide, 2) integrated in time air concentration of radionuclide within the surface layer of the atmosphere, 3) dry deposition of radionuclide on the underlying surface, and 4) wet deposition of radionuclide on the underlying surface. All these characteristics are given in a gridded domain having grid cells with a size of 0.5° × 0.5°, of latitude vs. longitude. Conditions and input parameters for the simulation runs are discussed in details by Baklanov et al. (2002a).

## 2.1.3. Statistical analysis of atmospheric transport and concentration patterns

Probabilistic analysis is one of the ways to estimate the likelihood of occurrence of one or more phenomena or events. The statistical analysis of trajectories might allow, from the probabilistic point of view, to evaluate the NRS possible impact on geographical regions or territories due to atmospheric transport. The statistical analysis of concentration/deposition fields might allow identifying the geographical areas at the highest risk of radionuclide contamination due to atmospheric transport and deposition (dry and/or wet) on the underlying surface.

The most interest in this study will be presented by the following indicators: the fast transport (FT) probability field, maximum reaching distance (MRD), maximum possible impact zone (MPIZ), and average integral concentration (AIC) field. Although other indicators such as simple characteristics of the NRS possible impact, atmospheric transport pathways, airflow patterns, precipitation factor, etc. might be considered for the

Title Page

Abstract

Introduction

Conclusions

References

Tables

Figures

◀

▶

◀

▶

Back

Close

Full Screen / Esc

Print Version

Interactive Discussion



nuclear risk sites (Mahura et al., 1999; Baklanov et al., 2002; Mahura, 2002; Mahura and Baklanov, 2002; Mahura et al., 2003).

For the construction of each of the mentioned indicators, a new gridded domain was built with the risk site in the centre of domain. For the construction of the FT, MPIZ, and MRD indicators based on trajectory modelling results, as input data, the latitude and longitude of trajectories (at 12 and 24 h of atmospheric transport) were used. For the construction of the AIC indicator based on dispersion modelling results, as input data, the 2-dimensional fields of the integrated in time air concentration of radionuclide (in each grid cell of domain) within the surface layer of the atmosphere were used.

### 2.1.3.1. Fast transport probability fields

The fast transport probability field (FTPF) indicates the probability of the air parcels movement during the first day of transport. Such indicator shows where air parcels might be located geographically after the first 12 and 24 h of atmospheric transport from the NRS location. In this approach, we analysed separately only trajectories terminated exactly after 12 and 24 h of transport. The areas with the highest occurrence of trajectory intersections with the grid domain cells will reflect territories under the highest possible impact from the nuclear risk site, if an accidental release occurred.

To construct the FT fields, the number of trajectory intersections with each grid cell of a new gridded domain was counted. Among all grid cells, the cell where the absolute maximum of trajectory intersections took place was identified as an “absolute maximum cell” (AMC). Because all trajectories start near the NRS region, to account for contribution into flow at the larger distances from the site, the area of maximum was extended to cells adjacent to AMC. For this purpose, the number of intersections in cells adjacent to AMC was compared, and additional cells (having less than 10% of difference between cells) were assigned. The new “area of maximums”, if isolines are drawn, will represent the area of the highest probability of the possible impact (AHPPI) from NRS. Assuming the value of 100% for this area, the rest could be re-calculated

Title Page

Abstract

Introduction

Conclusions

References

Tables

Figures

◀

▶

◀

▶

Back

Close

Full Screen / Esc

Print Version

Interactive Discussion

as percentage of AHPPI.

### 2.1.3.2. Maximum reaching distance and maximum possible impact zone Indicators

The maximum possible impact zone (MPIZ) indicator shows the boundaries of a territory on a geographical map with the highest probability of being reached by trajectories during the first day of transport from the site.

To construct the MPIZ indicator, all endpoints of 12-hours intervals of calculated trajectories only during the first day (i.e. at 12 and 24 h) of transport were counted in the cells of a new gridded domain. Similarly to the FTPF construction, both the AMC and AHPPI were identified. For the MPIZ indicator, it was assumed that the area of MPIZ includes all cells with an isoline of more than 90% of AHPPI, and an isoline of MPIZ was drawn through these cells.

The maximum reaching distance (MRD) indicator shows the farthest boundaries on the geographical map which might be reached during the first day of atmospheric transport by, at least, one trajectory originating over the risk site location.

To construct the MRD indicator, all endpoints of 12-hours intervals of calculated trajectories during the first day (i.e. at 12 and 24 h) of atmospheric transport were counted in the cells of a new gridded domain. An isoline of MRD was drawn through the grid cells of the domain where, at least, one trajectory intersected with the boundaries of the grid cell.

### 2.1.3.3. Average integral concentration fields

The dispersion modelling results can be analyzed in a similar manner to those for the trajectory modelling results. Further, the focus is on the integrated in time concentration of radionuclide. The average integral concentration (AIC) field is an average (at any given day of the analysed time period) integrated in time air concentration of

## Methodology for prediction of risk

A. Baklanov et al.

Title Page

Abstract

Introduction

Conclusions

References

Tables

Figures

◀

▶

◀

▶

Back

Close

Full Screen / Esc

Print Version

Interactive Discussion

radionuclide within the surface layer of the atmosphere. This type of the field shows the most probable geographical distribution of the radionuclide concentration near the surface due to atmospheric transport from the site.

To construct the AIC field, the total sum of daily continuous discrete releases of radioactivity at the site during the time period of interest (month) was counted in each grid cell of the domain. Then, an average value (or AIC) was obtained by division of values in each cell by the number of valid days (i.e. when meteorological data were available for operational dispersion modelling). An isoline of AIC was drawn through the grid cells of the domain with the equal orders of magnitude starting from  $10^{-1}$ .

Similarly to AIC, the average fields representing the dry, wet, and total deposition patterns due to atmospheric transport from the site could be simulated as suggested by AR-NARP (2001–2002), Baklanov et al. (2002a).

## 2.2. Approach for operation stage

At the operation stage, an approach, which includes two research tools, is suggested. These tools are the following: 1) 3-dimensional Danish Emergency Response Model for Atmosphere (DERMA), and 2) HIgh Resolution Limit Area Model (HIRLAM). Both models are operationally used and further developed by the Danish Meteorological Institute (DMI). The DMI-HIRLAM model (used as a numerical weather prediction – NWP-model) simulates the 3-dimensional fields for meteorological variables needed as input for the DERMA model. The DERMA model simulates the radionuclide transport, dispersion, and deposition for the hypothetical accidental release at the selected geographical locations of the submarine during the KNS operations. Further, the DERMA simulation results were used for comparison with the trajectory modelling results.

### 2.2.1. Operational emergency modelling

The Danish Emergency Response Model of the Atmosphere (DERMA) is used for the real-time modelling of possible contamination and consequences (cf. Fig. 2). The

Title Page

Abstract

Introduction

Conclusions

References

Tables

Figures

◀

▶

◀

▶

Back

Close

Full Screen / Esc

Print Version

Interactive Discussion

**Methodology for prediction of risk**

A. Baklanov et al.

[Title Page](#)[Abstract](#)[Introduction](#)[Conclusions](#)[References](#)[Tables](#)[Figures](#)[I◀](#)[▶I](#)[◀](#)[▶](#)[Back](#)[Close](#)[Full Screen / Esc](#)[Print Version](#)[Interactive Discussion](#)

© EGU 2003

model was developed at the Danish Meteorological Institute (DMI) for nuclear emergency preparedness purposes. DERMA is a 3-D Lagrangian long-range dispersion model using a puff diffusion parameterisation, particle-size dependent deposition parameterisations and radioactive decay (Sørensen, 1998; Sørensen et al., 1998; Baklanov and Sørensen, 2001). Earlier comparisons of simulations by the DERMA model vs. the ETEX experiment involving passive tracers gave very good results. 28 institutions from most European countries, USA, Canada and Japan contributed to the real-time model evaluation. Based on analyses from the first experiment, the DERMA model was emphasised as being very successful (Graziani et al., 1998). In general, the DERMA model can be used with different sources of NWP data, including the DMI-HIRLAM and ECMWF NWP models.

The main objective of the DERMA model is to predict the atmospheric transport, diffusion, deposition and radioactive decay of a radioactive plume within a range from about 20 km up to the global scale. For shorter distances the RIMPUFF local-scale model developed by the Risø NL (Mikkelsen et al., 1984, 1997) can be used. Both models are parts of the Danish Nuclear Preparedness System ARGOS (Hoe et al., 2000).

### 2.2.2. Weather forecast modelling

The DMI-HIRLAM high-resolution meteorological forecast (up to a few days) or analysed data (see Fig. 2.2.1: D-version: 0.05°, N- and E-versions: 0.15° or G-version: 0.45°, with 1 h time resolution) are used as input data for high-resolution trajectory or dispersion simulation in the DERMA model. The vertical DMI-HIRLAM model levels (currently in total 31 levels) are located at 33, 106, 188, 308, etc. meters for a standard atmosphere.

This model has been running operationally by DMI for the European and Arctic regions since 1990. The present DMI weather forecasting system is based on an extended version of the HIRLAM 4.7 model (Källén, 1996; Sass et al., 2002). The forecast model is a grid point model. The data assimilation is intermittent, and it is based on the

3-DVAR scheme. The operational system consists of four nested models called DMI-HIRLAM-G, -N, -E, and -D. These models differ by e.g. the horizontal resolutions and integration domains (cf. Fig. 2, the left panel). The NWP forecasting system is run on the NEC-SX6 supercomputer in connection with other DMI computers. The produced model level files are archived on the UNITREE Mass Storage System. Therefore, the DMI-HIRLAM data can be used in the operational mode or from the archives.

### 3. Results and Discussions

Using the suggested methodology an evaluation of possible risks and consequences from hypothetical accidental atmospheric releases of hazardous matter on example of the “Kursk” nuclear submarine (KNS) operation was realised. Simulation of possible consequences on the preparation and operational stages were done for most of the operation phases (see Table 1). However, for the analysis of the results and discussion let us consider the most important phases only.

At the preparation stage, the transport probability fields were constructed and analysed with respect to the locations of the sunken submarine and shipyards in Roslyakovo and Snezhnogorsk. At the operational stage, the following phases with the potential risk – “M” and “H”-levels (cf. Table 1) were considered: a) the lifting of KNS, b) the transportation to Roslyakovo, c) the setting to dry dock in the Roslyakovo shipyard; d) the decommissioning in the Snezhnogorsk shipyard – “Nerpa” (removal of the damaged missiles and the fuel).

Additionally, at the preparation stage, the earlier calculated transport probability fields for the nearby Kola Nuclear Power Plant were used for a preliminary investigation and for the site-sensitivity analysis of the probabilistic fields.

[Title Page](#)[Abstract](#)[Introduction](#)[Conclusions](#)[References](#)[Tables](#)[Figures](#)[◀](#)[▶](#)[◀](#)[▶](#)[Back](#)[Close](#)[Full Screen / Esc](#)[Print Version](#)[Interactive Discussion](#)

### 3.1. Fast transport probability fields during the first day of atmospheric transport

The fast transport probability fields (for both terms of 12 and 24 h) were constructed and analysed for two locations: the sunken Kursk NS and the Kola Nuclear Power Plant (i.e. over water and land surfaces, respectively). These fields provide useful information to evaluate the areas of the highest probability of the possible impact (AHPPI), if an accidental hypothetical release would have occurred. The fast transport probability fields (FTPF) during fall (three months combined: September, October, and November) are shown in Fig. 3 with the isolines drawn every 10% starting from 20.

Mahura et al. (2003) mentioned that during September-October, the westerly flow is dominant in the sunken NS region. After the first 12 h of atmospheric transport, the possibility of reaching the populated territories of the Murmansk region (Russia) was found to be low, and for the Nordic countries – minimal. At the end of the first day, the AHPPI boundaries were extended significantly in both meridional and latitudinal directions, covering the eastern territories of the Kola Peninsula. The main airflow tendencies during November–December were found to be similar, although in December the FTPF boundaries were also more farther extended to the west (reaching the northern Finland, Sweden, and Norway) compared with the fall months. Comparison with July–August showed that, from the atmospheric transport point of view, both September and October (when the operation for the Kursk NS in fact took place) were more suitable for the lifting and transportation of the submarine, because during summer, the largely populated territories of the Kola and Scandinavian Peninsulas were located inside the AHPPI zone. The monthly analysis of the fast atmospheric transport, from the probabilistic point of view, played a role of an indicator not only for the decision-making process in case of an accidental release, but also for the selection of the preferable time for the operation.

After transportation of the submarine (in October 2001) to the Roslyakovo shipyard, the KNS operation had continued (see Table 1) during the fall of 2001, and therefore, the fast transport patterns for two types of locations – over the water (KNS) and land

## Methodology for prediction of risk

A. Baklanov et al.

Title Page

Abstract

Introduction

Conclusions

References

Tables

Figures

◀

▶

◀

▶

Back

Close

Full Screen / Esc

Print Version

Interactive Discussion

(KNP) surfaces – should be further evaluated, because the Roslyakovo and Snezhnogorsk sites might represent a mixture of atmospheric transport patterns related to both geographical locations.

During fall, after the first 12 h of atmospheric transport, for both KNS and KNP the AHPPI boundaries are extended in the eastern direction over the Barents Sea and Kola Peninsula, respectively (Fig. 3). Although, the KNP site is located within the AHPPI boundaries, the KNS site is situated outside of the AHPPI boundaries. This is related to the fact that the wind speed over the open water is higher compared with the land surface, and hence, the flow propagates faster from the site region. For the KNS site, the area (enclosed by the lowest isoline of 20% of AHPPI) of the fast transport probability field is larger, and this field is more extended in the north-south direction compared with KNP. The NRS possible impact will be higher: in the northern Finland from KNP ( $\leq 90\%$  of AHPPI) compared with KNS ( $\leq 20\%$ ) as well as in Norway (Finmark County) from KNP ( $\leq 60\%$  of AHPPI) compared with KNS ( $\leq 35\%$ ).

Hence, it can be assumed by interpolating and averaging of the KNP and KNS FT probability fields that for the Roslyakovo and Snezhnogorsk shipyards, the most impacted areas outside of Russia could be the northern territories of Finland and Norway with the NRS possible impact varied in a range between 27–75% of AHPPI. It is very unlikely that the Swedish territories might be reached during the first 12 h of atmospheric transport from these sites.

During fall, at the end of the first day of atmospheric transport, for both sites – KNS and KNP – the AHPPI boundaries are shifted farther in the eastern direction from the sites by westerlies; and moreover, they represented by several maxima (which are extended more in the north-south direction compared with the west-east direction for the KNS and KNP sites, respectively). For both sites, by the end of the first day the Archangelsk Region (Russia) is at the highest risk due to atmospheric transport. Some peculiarities could be seen from the analysis of these fields. First, for the KNS site the FTPF boundaries (enclosed by 20% isoline) are more extended to the north of the site passing over  $75^\circ$  N, although for the KNP site it is southerly of this latitude. Second, the

**Methodology for prediction of risk**

A. Baklanov et al.

Title Page

Abstract

Introduction

Conclusions

References

Tables

Figures

◀

▶

◀

▶

Back

Close

Full Screen / Esc

Print Version

Interactive Discussion

**Methodology for prediction of risk**

A. Baklanov et al.

[Title Page](#)[Abstract](#)[Introduction](#)[Conclusions](#)[References](#)[Tables](#)[Figures](#)[I◀](#)[▶I](#)[◀](#)[▶](#)[Back](#)[Close](#)[Full Screen / Esc](#)[Print Version](#)[Interactive Discussion](#)

© EGU 2003

KNS FTPF is also significantly farther extended in the eastern direction compared with KNP. Third, for KNP there is the higher possibility (local maxima in Fig. 4) of reaching the southern populated territories of Finland compared to KNS, although for KNS there is an additional increase in probability of atmospheric transport in the NW sector of the site. As seen from FTPFs, in general, the atmospheric transport from the KNP site occurred in the E vs. SE sector, but for the KNS site – the NE vs. SE sector of the site.

Hence, similarly, interpolating and averaging the KNP and KNS FT probability fields it can be assumed that for the shipyards in Roslyakovo and Snezhnogorsk, the most impacted areas could be the Murmansk and Archangelsk Regions of Russia with the NRS possible impact varied in a range between 40–100% of AHPPI, although there might be such possibility also for the western and north-western territories of Finland.

It should be noted that it is possible to use simply a wind direction as an indicator of the atmospheric transport, but it is valid only on the local scale. It is also possible to use the climatological maps of baric topography, and although those give a general insight in the prevailing atmospheric transport over the large areas, they are not directly related to a particular site of concern. The statistical interpretation of probability fields represents the general climatological outlook of the possible atmospheric transport from a particular site. For a particular meteorological situation or episode, there may well be possibilities for transport in other directions.

### 3.2. Maximum possible impact and maximum reaching distance indicators

Similarly to the fast transport probability field (FTPF), the maximum reaching distance (MRD) and maximum possible impact zone (MPIZ) indicators during fall were analysed for both sites – Kursk NS and Kola NPP. The MPIZ indicator, as an integral characteristic, shows areas as well as boundaries with the highest probability of reaching by trajectories during the first day of transport. The MRD indicator shows the farthest boundaries on a geographical map, which might be reached during the first day, at least, by one trajectory originated over the site location. It should be noted that the shape of both indicators depends on the prevailing flow patterns.



**Methodology for prediction of risk**

A. Baklanov et al.

Title Page

Abstract

Introduction

Conclusions

References

Tables

Figures

◀

▶

◀

▶

Back

Close

Full Screen / Esc

Print Version

Interactive Discussion

© EGU 2003

During fall, the KNP MRD boundary is less extended in the northern direction compared with the KNS site (cf. Fig. 5). For KNP, this boundary is more farther extended over the Scandinavian Peninsula as well as farther to the south (reaching 55° N) compared with KNS, although for KNS this boundary is more extended in both eastern and south-eastern directions. The KNP MPIZ boundary reaches the KNS region, although it is not the same for the KNS MPIZ boundary. Moreover, the KNP MPIZ isoline underlines that the territories of the Murmansk Region and Karelia, and partially, the border region of Finland and parts of the White and Barents Seas are located within the areas of the highest NRS possible impact. For KNS, the north-western territories of the Kola Peninsula, Kanin Peninsula, and Barents Sea are enclosed by the MPIZ isoline. The estimation of areas enclosed by isolines of these indicators showed that during fall the MPIZ areas are equal to  $49 \cdot 10^4 \text{ km}^2$  and  $41 \cdot 10^4 \text{ km}^2$  for the KNS and KNP sites, respectively. The MRD area for the KNS site is almost 1.8 times higher compared to the KNP site (i.e.  $1588 \cdot 10^4 \text{ km}^2$  vs.  $895 \cdot 10^4 \text{ km}^2$ ).

### 3.3. Average integral concentration field

The average integral concentration field for a particular month might be used to calculate average dose characteristics due to inhalation from the passing radioactive cloud at any selected geographical location at any given day of a particular month. The summary monthly field might be used to calculate the monthly dose due to inhalation at any selected geographical location. The examples of averaged  $^{137}\text{Cs}$  integrated in time concentration fields after 1 day and 5 days of atmospheric transport from the KNS location in the Roslyakovo shipyard are shown in Figs. 6a and 6b, respectively. The daily discrete unit hypothetical release at the site during November 2001 was considered.

The area with the IAC highest orders of magnitude ( $\leq 1\text{e} + 2 \text{ Bq} \cdot \text{h}/\text{m}^3$ ) is extended in the NE-SW direction after the first day of atmospheric transport. For the five days of transport, the IAC area increased more in the NE sector compared with the SW sector from the site. Among the populated territories only the Kola Peninsula is affected.

**Methodology for prediction of risk**

A. Baklanov et al.

Title Page

Abstract

Introduction

Conclusions

References

Tables

Figures

◀

▶

◀

▶

Back

Close

Full Screen / Esc

Print Version

Interactive Discussion

© EGU 2003

Considering the medium IACs ( $1e + 2 - 1e + 0 \text{ Bq} \cdot \text{h}/\text{m}^3$ ) it should be noted that the Murmansk, Archangelsk, and Karelia Regions of Russia, the Finnmark County of Norway, northern and central territories of Finland, and partially the north-east border of Sweden became affected by the end of the first day of the atmospheric transport. For the five day transport, the propagation of the radioactive cloud is more extended in the NE sector over unpopulated territories of the Arctic Seas. The entire Finland and large areas of the Russian Northwest could expect the higher possibility of being reached by the contaminated cloud compared with Sweden and Norway. Moreover, during November the atmospheric transport dominates more by westerlies, and hence, the affected territories are located to the east of the site compared with the west of the site.

### 3.4. Operational dispersion modelling for different phases of the Kursk submarine operation

Although trajectory modelling for a multiyear period could provide valuable information for the preliminary evaluation of possible atmospheric transport from the risk site location, the real-time modelling is more useful in order to evaluate contamination and consequences of possible accidental releases.

In general, for the selection of the specific case studies we used simultaneously several criteria (Baklanov, 2000; Baklanov and Mahura, 2001). Among these criteria the most important are direction of atmospheric transport of an accidental release to the region of interest, possibility of removal over the study region during transport of a release, relatively short travel time from the NRS location and large coverage territories by the radioactive plume.

In this study, the possible contamination of the environment using the DERMA and DMI-HIRLAM models in forecasting mode was estimated. As a first approximation, the discrete unit hypothetical release (DUHR) of  $10^{11} \text{ Bq/s}$  of  $^{137}\text{Cs}$  which occurred daily during 6 h at the KNS location was considered. For all specific cases the simulation of the radionuclide surface air concentration ( $\text{Bq}/\text{m}^3$ ), wet and dry deposition ( $\text{Bq}/\text{m}^2$ )

fields was performed.

### 3.4.1. The lifting phase

In our simulation, starting from 24 September 2001, this DUHR occurred daily between 12:00 and 18:00 UTC. During 24 September and 17 October 2001, the simulation of the radionuclide concentration ( $\text{Bq/m}^3$ ), wet and dry deposition ( $\text{Bq/m}^2$ ) fields was performed. For modelling at this phase of the operation the geographical co-ordinates of KNS in the Barents Sea were used. It should be noted that on the local scale, the concentration fields are important input to calculation of doses for the population as the first consequences of accidental releases at risk sites. On the regional scale, the wet and dry deposition fields are important input to calculation of long-term consequences through the food chains. These fields underline boundaries of the geographical territories under the possible impact of accidental releases at risk sites.

From the total number of calculated operational dispersion cases (24), there are 19 (79%) cases showing transport toward eastern directions (westerly flows). It is in a good agreement with the results of the isentropic trajectory modelling. It reflected the fact that during September and October the westerly flows are dominant, as well as the fact that AHPPI is located to east from the sunken submarine location. Atmospheric transport to west occurred only in two cases, as well as transport to south – two cases. We should mention also that only one case – a hypothetical accidental release occurred at 3 October 2001 – showed complex atmospheric transport and deposition patterns (cf. Fig. 7).

For this case, during the first hours after the hypothetical accidental release at KNS, the westerly flows dominate in the transport pattern. Starting at 4 October 2001, 06 UTC there is a tendency of easterly flows, and this tendency increases faster in comparison with the westerly flow. Starting at 5 October 2001, 09:00 UTC, transport in the eastern direction again becomes dominant, and transport toward west diminishes. This complexity depends on the splitting of the initial radioactive cloud after the first several hours, and it is due to significant synoptical activity in the region of interest. It should

## Methodology for prediction of risk

A. Baklanov et al.

Title Page

Abstract

Introduction

Conclusions

References

Tables

Figures

◀

▶

◀

▶

Back

Close

Full Screen / Esc

Print Version

Interactive Discussion

be noted that if consider the total unit release of 1 Bq of  $^{137}\text{Cs}$  than the maximum total deposition in the source local zone will have a deposition fraction of  $10^{-10}$  Bq/m<sup>2</sup>, over the Kola Peninsula –  $10^{-11}$ , over the Archangelsk Region –  $10^{-12}$ , and over the Norwegian-Swedish border regions –  $10^{-13}$ .

### 5 3.4.2. The transportation phase

Starting from 8 October 2001 (i.e. during the KNS transportation through the Barents Sea and Kola Bay to the Roslyakovo shipyard), the DUHR occurred daily between 09:00 and 15:00 UTC during 8–17 October 2001.

10 During the KNS transportation phase to Roslyakovo, we used approximate co-ordinates of the proposed route, and at the final phase – co-ordinates of the Roslyakovo shipyard. The choice of the co-ordinates as a function of time is very important in such studies, especially for the local-scale risk analysis. However, it is very problematic to calculate coordinates precisely during transportation with different speeds, uncertain route, etc. Hence, a new idea to use GPS in operational simulation for the moving  
15 risk sites is suggested by the ENSEMBLE Project (Galmarini, 2001) and planned to be used in future.

For this phase, from the total numbers of calculated cases most of the cases showed transport toward northern or eastern directions (southerly or westerly flows) to unpopulated areas of the Arctic Ocean seas. Only two cases showed the northerly and north-westerly flows to the populated areas of the Murmansk and Archangelsk Regions of  
20 Russia. In example, shown in Fig. 8, during the first half of the day the atmospheric transport occurred in the western direction and the radioactive plume passed over the northern territories of Norway. Among all considered cases, this case was only one showing transport over the Norwegian territory. This plume was later transported to  
25 the north and east passing over the Barents Sea and Novaya Zemlya Archipelago.

For the total unit release of 1 Bq of  $^{137}\text{Cs}$ , the maximum deposition in the source local zone has a fraction of  $10^{-11}$  and  $10^{-10}$  Bq/m<sup>2</sup> for the dry and wet deposition,

Title Page

Abstract

Introduction

Conclusions

References

Tables

Figures

◀

▶

◀

▶

Back

Close

Full Screen / Esc

Print Version

Interactive Discussion

**Methodology for prediction of risk**

A. Baklanov et al.

Title Page

Abstract

Introduction

Conclusions

References

Tables

Figures

◀

▶

◀

▶

Back

Close

Full Screen / Esc

Print Version

Interactive Discussion

© EGU 2003

respectively. The level of deposition in the Russian-Norwegian border regions was one order of magnitude lower than the level of deposition around the KNS site. However, the dry deposition decreases faster with distance compared with the wet deposition, and the tail of the wet deposition field with a fraction of  $10^{-11}$  extended for a long distance from the site (up to 1000 km).

### 3.4.3. The decommission phase in Roslyakovo

After the transportation through the Kola Bay to the Roslyakovo harbour, the submarine was relocated from the “Giant-4” barge and set in the dry dock of the Roslyakovo shipyard during the second and third decades of October 2001. Then, the first step of the KNS decommissioning phase started in the Roslyakovo shipyard, and it included the removal of missiles. One specific case of DUHR of  $^{137}\text{Cs}$  at 16 October 2001 is considered.

Figure 9 shows the  $^{137}\text{Cs}$  dry and wet deposition fields at 18 October 2001, 21:00 UTC. During the first day after the hypothetical accidental release at KNS, the westerly and north-westerly flows dominate in the transport pattern. Starting at 17 October 2001 there is a tendency of northerly flows, and later of the north-westerly flow again. The plume reached the Archangelsk Region with the deposition fraction of one-two orders of magnitude lower than the deposition level in the area of the KNS release. The deposition fraction over the St.Petersburg Region is of three and four orders of magnitude lower compared with the KNS release site for the dry and wet deposition, respectively.

### 3.4.4. The decommission phase in Snezhnogorsk

Let us consider the potential risk of airborne contamination for DUHR of  $^{137}\text{Cs}$  during the KNS operation phases #10 and #12, which include the removal of six damaged missiles and nuclear fuel from KNS in the “Nerpa” dry dock during July–October 2002.

The hypothetical release from the site started at 10 September 2002, 12:00 UTC,

and it continued during 1 h with the heights of the primary radioactive plume between 0–500 m. The remaining model input data and conditions are similar to the previous case studies.

Figure 10 presents dynamics of the weather situation based on the DMI-HIRLAM numerical weather forecast for the region of interest during 10–13 September 2002. The wind field maps shown in Fig. 10 represent the forecast by the E-version (15 × 15 km horizontal resolution) and G-version (45 × 45 km horizontal resolution) of the DMI-HIRLAM model. As shown in Fig. 10a, the higher resolution version of the model has a limitation of the modelling domain close to the KNS location, and hence, depending on the wind direction from the site the E- or G-version for the dispersion modelling could be used.

Figure 11 shows the calculated air concentration ( $\text{Bq/m}^3$ ) in the mixing layer at different times after the beginning of DUHR of  $^{137}\text{Cs}$  from the risk site. The integrated in time surface air concentration ( $\text{Bq} \times \text{h/m}^3$ ) and ground-contamination (total deposition as the sum of dry and wet depositions, in  $\text{Bq/m}^2$ ) four days after the release started are shown in Fig. 12.

During the first day, the radioactive plume is transported slowly over the Kola Peninsula and Karelia to the south, due to low wind velocity within the boundary layer for this meteorological situation. On the second day, the plume is also extended to the north over the Barents Sea. An intensive precipitation in the first days after the release gives a large area of maximal deposition of radionuclides over the Kola Peninsula and surrounding areas. On the third day, the plume continued to move in the south-east and east direction from the site, but concentration decreased fastly and considerably.

### 3.4.5. Evaluation of possible consequences

It should be stressed again that we do not link the hypothetical accident releases considered in the following analysis with the “Kursk” submarine case. In our analysis, we simply discuss possible consequences and their scales after the most severe hypothetical accident with a ship nuclear reactor. Moreover, it should be noted that all

---

**Methodology for prediction of risk**

A. Baklanov et al.

---

Title Page

Abstract

Introduction

Conclusions

References

Tables

Figures

◀

▶

◀

▶

Back

Close

Full Screen / Esc

Print Version

Interactive Discussion

completed high and medium potential risk level phases/actions of the KNS operation were performed successfully, and none of them involved any radioactive contamination or real risk for the population and the environment.

As it was mentioned above, the simulations were done for a discrete unit hypothetical release of  $^{137}\text{Cs}$ . However, any expert can easily recalculate the concentration and deposition fields for any particular release value.

Although the ship reactor accidents may lead to serious environmental consequences, some studies (e.g. NACC, 1998) indicate that any potential naval reactor accident will not be nearly as severe as the Chernobyl accident. Some calculation of airborne transport, deposition, and exposure had been made based on an assumed release of 1 PBq of  $^{137}\text{Cs}$  (NACC, 1998; Bergman et al., 1998). It is not obvious that this amount would actually be released in an accident, even if it is available in the core. Moreover, the relative uncertainty of the release is estimated to be a factor of ten. The maximum content of  $^{137}\text{Cs}$  in the first and second generation of the Russian ship reactors is estimated to 5 PBq (Gussgard, 1995), while 10 PBq may be accumulated during operation of a typical modern ship reactor (i.e. with a power level slightly less than 200 MW). The KNS core inventory was not available in this study. However, a rough guess of the Bellona experts based on the known inventories of other submarines (Gerdes et al., 2001; Bellona, 2001) gives 6.2 PBq of  $^{137}\text{Cs}$  and 5.6 PBq of  $^{90}\text{Sr}$ .

Our calculation (based on Figs. 9 and 12) for the total unit release (1 Bq) case indicates that the large areas of the Northwest Russia (excluding the Kola Peninsula) could obtain deposition of a fraction of the order of  $10^{-13} \text{ Bq/m}^2$ . This corresponds to a deposition of  $100 \text{ Bq/m}^2$  per 1 PBq of airborne release of  $^{137}\text{Cs}$  in the accident, i.e. the level used in the NACC, 1998 study. On the Kola Peninsula the higher deposition density (one to two orders of magnitude) might be expected compared with the Northwest Russia. In our case, 1 PBq of  $^{137}\text{Cs}$  airborne release corresponds to  $1\text{--}10 \text{ kBq/m}^2$  and up to  $50 \text{ kBq/m}^2$  on the Kola Peninsula vs. local scale close to the release site.

For Scandinavia, the direct deposition of  $^{131}\text{I}$  or  $^{137}\text{Cs}$  on pasture and crops at levels

Methodology for prediction of risk

A. Baklanov et al.

Title Page

Abstract

Introduction

Conclusions

References

Tables

Figures

◀

▶

◀

▶

Back

Close

Full Screen / Esc

Print Version

Interactive Discussion

**Methodology for prediction of risk**

A. Baklanov et al.

Title Page

Abstract

Introduction

Conclusions

References

Tables

Figures

◀

▶

◀

▶

Back

Close

Full Screen / Esc

Print Version

Interactive Discussion

© EGU 2003

falling below 1 kBq/m<sup>2</sup> is not likely leading to restrictions in normal agricultural practice or formal acceptance for commercial use of the food-products (Bergman et al., 1998). The concentration in reindeer in the Northern Fennoscandia is high, when feeding during winter on lichens exposed to fallout of radioactive caesium (<sup>134</sup>Cs and <sup>137</sup>Cs).

5 The ratio between activity concentration in the reindeer meat and deposition density will be close to 1 kg/m<sup>2</sup> in the latter half of the first winter season after the fallout (Bergman and Ågren, 1999). This implies contamination about one order of magnitude higher than concerning direct deposition in the sensitive food-chain of grass-cow-milk. Intake of radioactive caesium in groups or populations consuming much reindeer meat is expected to be high.

10 Assuming a release of 1 PBq of <sup>137</sup>Cs and following Bergman et al., 1998, the levels of this radionuclide attained in reindeer meat are expected to be: 1) 1 kBq/kg in large areas on the Kola Peninsula affected by deposition, and 2) one order of magnitude higher over some smaller areas ranging within a hundred kilometres from the site of release.

#### 4. Conclusions

In this study, a combination of several research tools to evaluate the possible atmospheric transport, contamination, and consequences as a result of a discrete unit hypothetical release at a nuclear risk site was used. Among these tools are: 1) isentropic trajectory modelling for a multiyear period; 2) atmospheric dispersion modelling of radioactivity releases for a long-term period, 3) operational emergency response modelling based on numerical weather prediction model data, and 4) statistical analyses of trajectory and dispersion modelling results. The combined use of the first, second and fourth tools could be applied (as the first approach) during the preparation stage, and the third tool (as the second approach) – during the operation stage. The suggested methodology is tested on an example of the most important phases of the “Kursk” nuclear submarine operation.



**Methodology for prediction of risk**

A. Baklanov et al.

Title Page

Abstract

Introduction

Conclusions

References

Tables

Figures

◀

▶

◀

▶

Back

Close

Full Screen / Esc

Print Version

Interactive Discussion

© EGU 2003

The temporal variability of several probabilistic indicators (fast transport probability fields, maximum reaching distance, maximum possible impact zone, and average integral concentration of  $^{137}\text{Cs}$ ) showed that the Fall of 2001 was the most appropriate time for the beginning of the operation. These indicators allowed to identify the most probably impacted geographical regions and territories. In cases of atmospheric transport toward the most populated areas, the forecasts of possible consequences during phases of the high and medium potential risk levels (lifting, transportation, and decommissioning of the submarine) based on a unit hypothetical release were performed. The analysis showed that the possible deposition fractions of  $10^{-11}$  over the Kola Peninsula, and  $10^{-12} - 10^{-13}$  for the remote areas of the Scandinavia and Northwest Russia could be observed.

It is suggested that the combined use of both approaches for the estimation of possible consequences of accidental releases at nuclear risk sites is more valuable. From one side, during the preparation stage – the trajectory and dispersion modelling for the long-term period, and probabilistic fields analysis could provide preliminary information about possible directions and probabilities of atmospheric transport from the risk site locations. From other side, during the operation stage – the real-time modelling could provide detailed current and forecasted information about the spatial and temporal distributions of concentration, wet and dry deposition of radionuclides of key importance. It is concluded that the use of both approaches provides the most valuable basis for risk analysis.

Finally, it should be noted that although the “Kursk” nuclear submarine was selected as an example for this study, the suggested methodology could be used successfully for any object of potential nuclear, chemical or biological danger.

*Acknowledgement.* The authors are grateful to L. Laursen (Danish Meteorological Institute), O. Rigina (Geographical Institute of Copenhagen University, Denmark), R. Bergman (Swedish Defence Research Authority, Umeå), Sergey Morozov (Kola Science Center, Russian Academy of Sciences, Apatity, Russia), F. L. Parker (Vanderbilt University, Nashville, TN, USA), K. Compton (International Institute for Applied Systems Analysis, Laxenburg, Austria), B. Segerståhl (Thule

Institute of University of Oulu, Finland), J. Merrill (University of Rhode Island, RI, USA), I. Kudrik (Bellona) for collaboration and constructive comments.

The computer facilities at the Danish Meteorological Institute (DMI, Copenhagen, Denmark), the International Institute for Applied Systems Analysis (IIASA, Laxenburg, Austria), and the National Center for Atmospheric Research (NCAR, Boulder, USA) have been used in this study. The meteorological data archives from the NCAR and DMI facilities were used as input to the isentropic trajectory and operational dispersion modelling.

Thanks to the computer consulting services at DMI, IIASA, and NCAR for the collaboration, computer assistance, and advice. Financial support of this study included the grants of the Nordic Arctic Research Programme (NARP), the Nordisk Forskerutdanningsakademi (NorFA), and US Department of Energy (US DOE).

## References

AR-NARP: Atmospheric Transport Pathways, Vulnerability and Possible Accidental Consequences from the Nuclear Risk Sites in the European Arctic (Arctic Risk). Project of the Nordic Arctic Research Program (NARP). Arctic Risk Project Official web-site: <http://www.dmi.dk/f+u/luft/eng/arctic-risk/main.html>, 2001–2003.

Baklanov, A. : Modelling of episodes of atmospheric transport and deposition: Hypothetical nuclear accidents in North-West Russia, in: Nuclear Risks, Environmental and Development Cooperation in the North of Europe, CERUM, University of Umeå, Sweden, ISBN 91-7191-789.6, 65–80, 2000.

Baklanov, A. and Mahura, A.: Atmospheric Transport Pathways, Vulnerability and Possible Accidental Consequences from Nuclear Risk Sites: Methodology for Probabilistic Atmospheric Studies. DMI Scientific Report #01-09, ISBN: 87-7478-391-2, Danish Meteorological Institute, Denmark, Fall 2001, 45, 2001.

Baklanov, A. and Sørensen, J. H.: Parameterisation of radionuclide deposition in atmospheric long-range transport modelling, Physics and Chemistry of the Earth:(B), 26, 10, 787–799, 2001.

Baklanov, A., Mahura, A., Jaffe, D., Thaning, L., Bergman, R., and Andres, R.: Atmospheric Transport Patterns and Possible Consequences for the European North after a Nuclear Accident, Journal of Environment Radioactivity, 60, 23–48, 2002.

## Methodology for prediction of risk

A. Baklanov et al.

Title Page

Abstract

Introduction

Conclusions

References

Tables

Figures

◀

▶

◀

▶

Back

Close

Full Screen / Esc

Print Version

Interactive Discussion

Baklanov, A., Mahura, A., Sørensen, J. H., and Rigina, O.: Methodology for Risk Analysis based on Atmospheric Dispersion Modelling from Nuclear Risk Sites, DMI Scientific Report #02-16, 58, 2002a.

Bellona: <http://www.bellona.no/>, 2001.

5 Bergman, R. and Baklanov, A.: Radioactive sources in main radiological concern in the Kola-Barents region. FRN/FOA Publication, Stockholm, 80, 1998.

Bergman, R., Thaning, L., and Baklanov, A.: Site-sensitive hazards of potential airborne radioactive release from sources on the Kola Peninsula. FOA report: FOA-R00717-861-SE, 14, 1998.

10 Bergman, R. and Ågren, G.: Radioecological Characteristics of Boreal or Sub-Arctic Environments in Northern Sweden: focus on long-term transfer of radioactive deposition over food-chains. In: The 4th International conference on Environmental Radioactivity in the Arctic, Edinburgh, Scotland, 20–23 Sept., 91–94, 1999.

Galmarini, S.: Personal communication, ENSEMBLE project meeting, 12 December 2001, JRC, Ispra, Italy, 2001.

15 Gerdes, R., Karcher, M., Kauker, F., and Köberle, C.: Predicting the spread of radioactive substances from the Kursk, Eos, Transactions, AGU, 82, 23, 253, 256–257, 2001.

Graziani, G., Klug, W., and Moksa, S. (Eds.): Real-Time Long-Range Dispersion Model Evaluation of the ETEX First Release, Joint Research Centre, EU, Luxemburg, 1998.

20 Gussgard, K.: Is spent nuclear fuel at the Kola Coast and dumped in waters a real danger? In: P. Strand and A. Cooke (Eds.): Environmental Radioactivity in the Arctic, Østerås, 400–404, 1995.

Findings: Investigation results of the “Kursk” NS disaster reasons. Official Public Report of the Department of Justice of the Russian Federation. 22 July 2002, Moscow, 2002.

25 Hoe S., Müller, H., and Thykier-Nielsen, S.: Integration of dispersion and radio ecological modelling in ARGOS NT. To appear in: Proceedings of IRPA 10, Tenth International Congress of the International Radiation Protection Association, Hiroshima, Japan, May 14–19, 2000.

ITAR-TASS: Kursk Submarine to be Scrapped in Autumn – Commander, ITAR-TASS News Agency, July 17, 2002.

30 Kursk-web-site: An operation to lift the nuclear submarine KURSK. Official information channel: <http://kursk.strana.ru> or <http://www.kursk141.org/>, 2001–2002.

Källén, E. (Ed.): HIRLAM documentation manual, System 2.5, SMHI, Norrköping, Sweden, 1996.

---

**Methodology for prediction of risk**

A. Baklanov et al.

---

Title Page

Abstract

Introduction

Conclusions

References

Tables

Figures

◀

▶

◀

▶

Back

Close

Full Screen / Esc

Print Version

Interactive Discussion

**Methodology for prediction of risk**

A. Baklanov et al.

Title Page

Abstract

Introduction

Conclusions

References

Tables

Figures

◀

▶

◀

▶

Back

Close

Full Screen / Esc

Print Version

Interactive Discussion

© EGU 2003

- Lifting: Safety passport of work on the operation “Lifting”; Ecological safety passport of work on the operation “Lifting”. Moscow, <http://kursk.strana.ru/dossier/997885469.html>, 2001.
- Mahura, A., Andres, R., and Jaffe, D.: Atmospheric transport patterns from the Kola Nuclear Reactors. CERUM northern Studies Working Paper, 24, 33, 2001.
- 5 Mahura, A. and Baklanov, A.: Probabilistic Analysis of Atmospheric Transport Patterns from Nuclear Risk Sites in Euro-Arctic Region, Danish Meteorological Institute, DMI Scientific Report #02-15, 87, 2002.
- Mahura A., Jaffe, D., Andres, R., and Merrill, J.: Atmospheric transport pathways from the Bilibino nuclear power plant to Alaska, Atmospheric Environment, 33/30, 5115–5122, 1999.
- 10 Mahura, A.: Assessment of Impact of Russian Nuclear Fleet Operations on Russian Far Eastern Coastal Regions. IIASA Interim Report: IR-02-004, International Institute for Applied Systems Analysis, Austria, 76, 2002.
- Mahura, A., Baklanov, A., and Sørensen, J. H.: Methodology for evaluation of possible consequences of accidental atmospheric releases of hazardous matter, Journal of Radiation Protection Dosimetry, 103, 2, 131–139, 2003.
- 15 Matishov, G. G., Matishov, D. G., Namjatov, A. E., Smith, J. N., Carroll, J., and Dahle, S.: Radioactivity near the sunken submarine “Kursk” in the southern Barents Sea, Envir. Science and Technol., 8, 9, 1919–1922, 2002.
- Merrill, J., Bleck, R., and Boudra, D. B.: Techniques of Lagrangian Trajectory Analysis in Isentropic Coordinates, Monthly Weather Review, 114, 571-581, 1985.
- 20 Mikkelsen, T., Larsen, S. E., and Thykier-Nielsen, S.: Description of the Risø puff diffusion model, Nuclear Technology, 67: 56–65, 1984.
- Mikkelsen, T., Thykier-Nielsen, S., Astrup, P., Santabarbara, J. M., Sørensen, J. H., Rasmussen, A., Robertson, L., Ullerstig, A., Deme, S., Martens, R., Bartzis, J. G., and Pasler-Sauer, J.: MET-RODOS: A comprehensive atmospheric dispersion module, Radiat. Prot. Dosim., 73, 45–56, 1997.
- 25 NACC: Cross-border environmental problems emanating from defence-related installations and activities, Phase 2: 1995–1998, Report no 223, North Atlantic Treaty Organisation, 1998.
- Sass, B. H., Nielsen, N. W., Jørgensen, J. U., Amstrup, B., Kmit, M., and Mogensen, K.: The operational HIRLAM system 2002-version, Danish Meteorological Technical Report 02–05, Copenhagen, Denmark, 2002.
- 30 Sørensen, J. H.: Sensitivity of the DERMA Long-Range Gaussian Dispersion Model to Meteorological Input and Diffusion Parameters, Atmospheric Environment, 32, 4195–4206, 1998.

Sørensen, J. H., Rasmussen, A., Ellermann, T., and Lyck, E.: Mesoscale Influence on Long-range Transport; Evidence from ETEX Modelling and Observations, Atmospheric Environment, 32, 4207–4217, 1998.

- 5 Stohl, A.: Computation, accuracy and applications of trajectories – A review and bibliography, Atmospheric Environment, 32, 947–966, 1998.

---

**Methodology for prediction of risk**

A. Baklanov et al.

---

Title Page

Abstract

Introduction

Conclusions

References

Tables

Figures

◀

▶

◀

▶

Back

Close

Full Screen / Esc

Print Version

Interactive Discussion

**Table 1.** Potential risk level ranging for the “Kursk” nuclear submarine operation phases

#	Phases/actions <sup>(*)</sup>	Phase date <sup>(*)</sup>	Potential risk level
1	Accident and sinking	12 Sept. 2000	H/L <sup>a</sup>
2	Lifting preparation	16 July–6 Oct. 2001	L
3	Lifting submarine	7–8 Oct. 2001	M
4	Transportation to Roslyakovo	8–10 Oct. 2001	M
5	Setting in dry dock of Roslyakovo	21–22 Oct. 2001	L
6	Missiles removal	Feb. 2002	H/U <sup>a</sup>
7	Transportation to Snezhnogorsk	26–27 April 2002	L
8	Setting in dry dock of Nerpa	27–30 April 2002	L
9	1 <sup>st</sup> compartment parts lifting	end of May–20 June 2002	N <sup>b</sup>
10	6 Damaged missiles removal	July 2002	M/U <sup>a</sup>
11	1 <sup>st</sup> compartment blasting	8–9 Sept. 2002	N <sup>b</sup>
12	Nuclear fuel removal	Oct.–Nov. 2002	M
13	Reactor removal	Nov. 2002	L
14	Transportation of reactor and fuel	after Dec. 2002	L <sup>c</sup>
15	Damaged missiles blasting	15 Oct.–15 Nov. 2002	N <sup>b</sup>
16	Scrapping submarine	after Dec. 2002	N

(\*) All the information was received from the official Kursk Information Web-Site: (Kursk-web-site, 2001–2002).

Risk categories: H – high, M – middle, L – low, U – unknown, N – no risk,

Comments: <sup>a</sup> before and after first information received, <sup>b</sup> local non-nuclear risk, <sup>c</sup> if a crash or terror act.

## Methodology for prediction of risk

A. Baklanov et al.

Title Page

Abstract

Introduction

Conclusions

References

Tables

Figures

◀

▶

◀

▶

Back

Close

Full Screen / Esc

Print Version

Interactive Discussion

© EGU 2003

Methodology for prediction of risk

A. Baklanov et al.

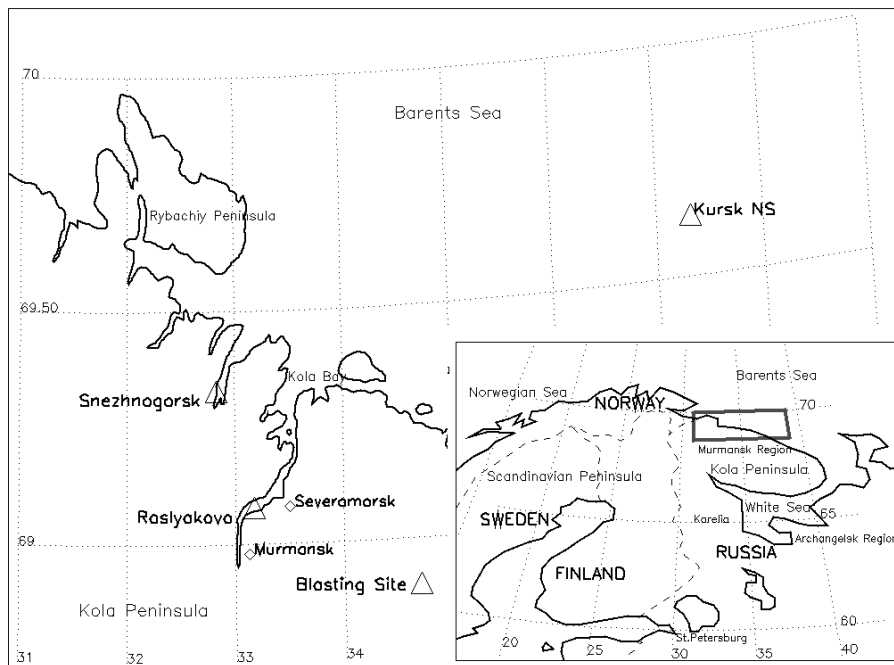


**Fig. 1.** Locations of the sunken nuclear submarine “Kursk”, the shipyard in Roslyakovo, the “Nerpa” shipyard in Snezhnogorsk, and the blasting site.

Title Page

Abstract

Introduction

Conclusions

References

Tables

Figures

◀

▶

◀

▶

Back

Close

Full Screen / Esc

Print Version

Interactive Discussion

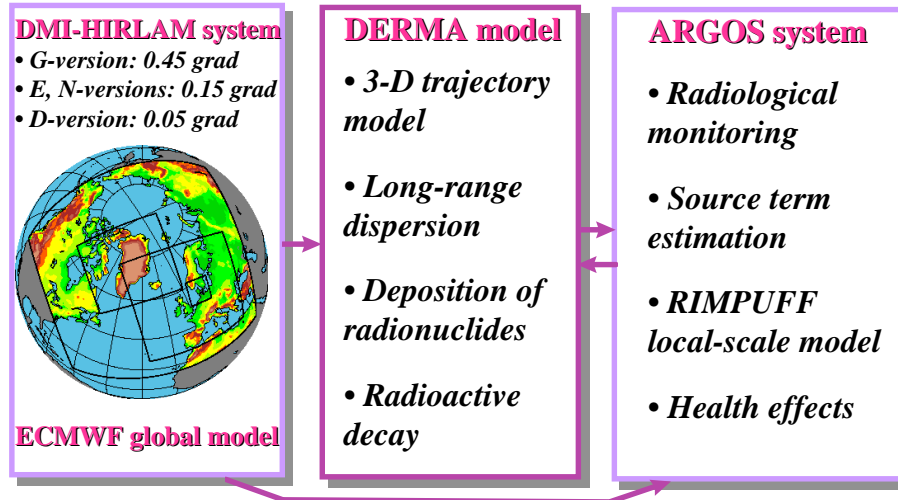


Fig. 2. Structure of the Danish nuclear emergency preparedness long-range modelling system.

Title Page	
Abstract	Introduction
Conclusions	References
Tables	Figures
◀	▶
◀	▶
Back	Close
Full Screen / Esc	
Print Version	
Interactive Discussion	



**Methodology for  
prediction of risk**

A. Baklanov et al.

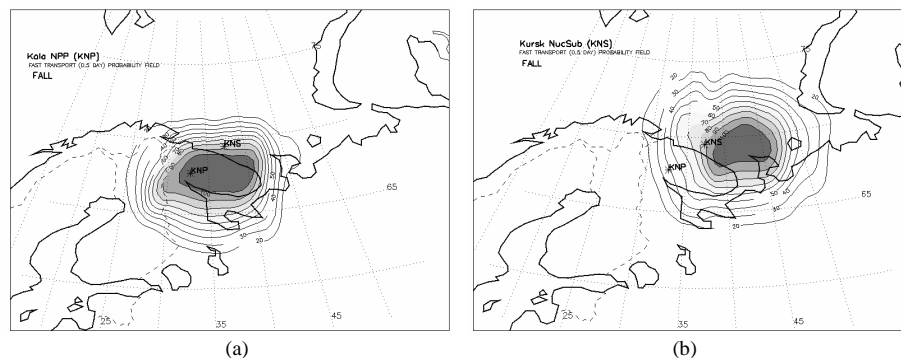


**Fig. 3.** Fast transport probability fields after 12 h of atmospheric transport during fall for the (a) Kola NPP and (b) Kursk NS.

[Title Page](#)[Abstract](#)[Introduction](#)[Conclusions](#)[References](#)[Tables](#)[Figures](#)[I◀](#)[▶I](#)[◀](#)[▶](#)[Back](#)[Close](#)[Full Screen / Esc](#)[Print Version](#)[Interactive Discussion](#)

© EGU 2003

Methodology for  
prediction of risk

A. Baklanov et al.

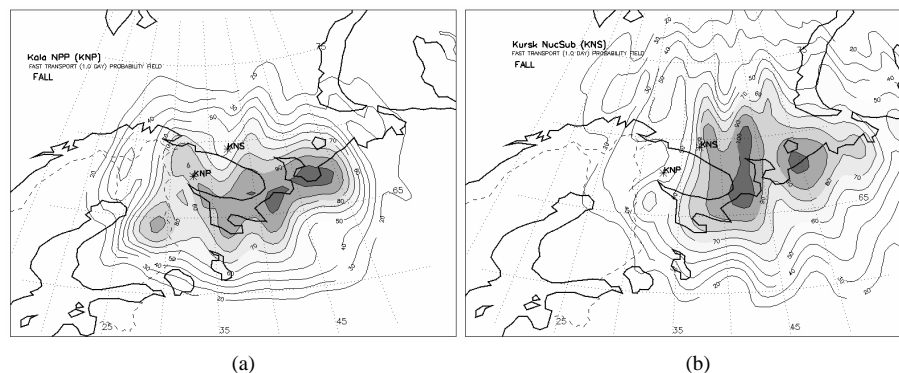


**Fig. 4.** Fast transport probability fields after 24 h of atmospheric transport during fall for the (a) Kola NPP and (b) Kursk NS.

[Title Page](#)[Abstract](#)[Introduction](#)[Conclusions](#)[References](#)[Tables](#)[Figures](#)[I◀](#)[▶I](#)[◀](#)[▶](#)[Back](#)[Close](#)[Full Screen / Esc](#)[Print Version](#)[Interactive Discussion](#)

© EGU 2003

Methodology for  
prediction of risk

A. Baklanov et al.

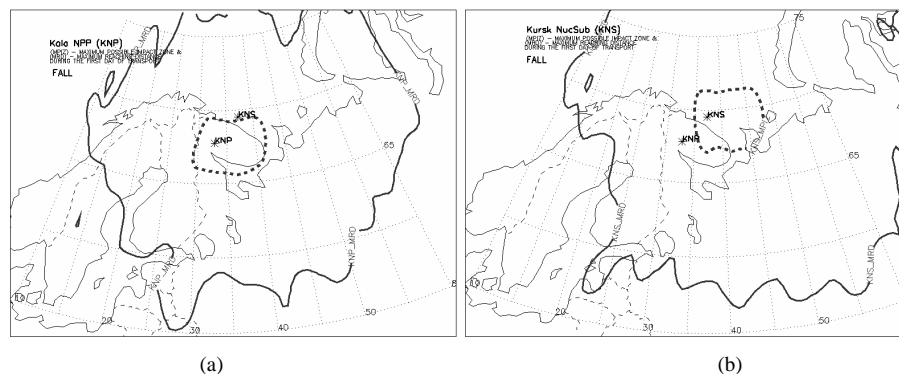


**Fig. 5.** Boundaries of the maximum reaching distance (—MRD—) and maximum possible impact zone (—MPIZ—) indicators during fall for the **(a)** Kola NPP and **(b)** Kursk NS.

[Title Page](#)[Abstract](#)[Introduction](#)[Conclusions](#)[References](#)[Tables](#)[Figures](#)[◀](#)[▶](#)[◀](#)[▶](#)[Back](#)[Close](#)[Full Screen / Esc](#)[Print Version](#)[Interactive Discussion](#)

© EGU 2003

**Methodology for  
prediction of risk**

A. Baklanov et al.

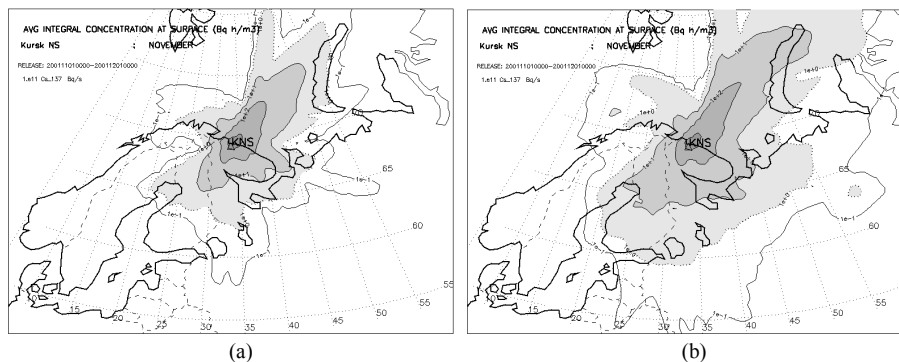


**Fig. 6.** Average integral concentration at surface field during November 2001 for the “unit discrete hypothetical release” of  $^{137}\text{Cs}$  during November 2001 after (a) 1 day and (b) 5 days of atmospheric transport from the Kursk NS site.

[Title Page](#)[Abstract](#)[Introduction](#)[Conclusions](#)[References](#)[Tables](#)[Figures](#)[◀](#)[▶](#)[◀](#)[▶](#)[Back](#)[Close](#)[Full Screen / Esc](#)[Print Version](#)[Interactive Discussion](#)

© EGU 2003

Methodology for  
prediction of risk

A. Baklanov et al.

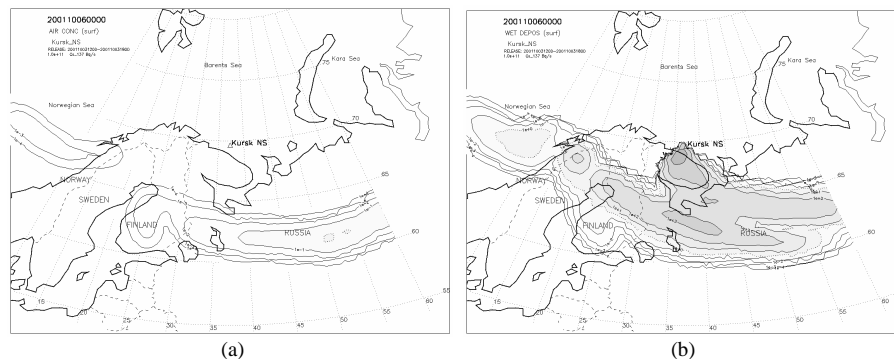


**Fig. 7.** Specific case of 3 October 2001 for the “unit discrete hypothetical release” of  $^{137}\text{Cs}$  at the accident location: **(a)** surface air concentration and **(b)** wet deposition fields at 6 October 2001, 00:00 UTC.

[Title Page](#)[Abstract](#)[Introduction](#)[Conclusions](#)[References](#)[Tables](#)[Figures](#)[◀](#)[▶](#)[◀](#)[▶](#)[Back](#)[Close](#)[Full Screen / Esc](#)[Print Version](#)[Interactive Discussion](#)

© EGU 2003

Methodology for  
prediction of risk

A. Baklanov et al.

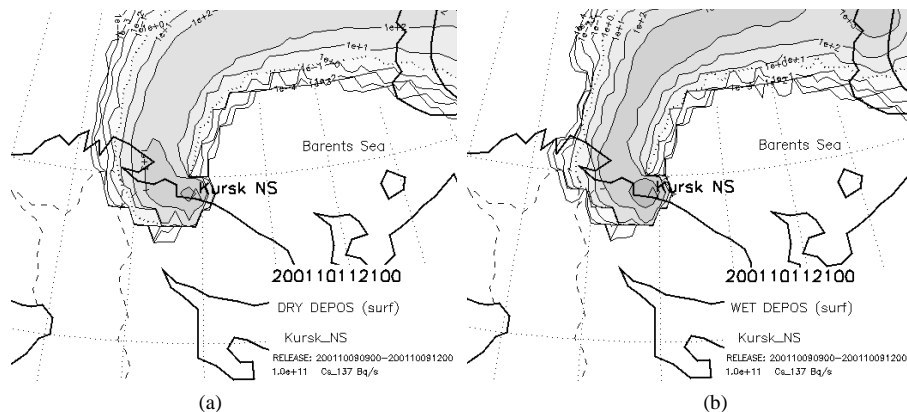


**Fig. 8.** Specific case of 9 October 2001 for the “unit discrete hypothetical release” of  $^{137}\text{Cs}$  during the submarine transportation: **(a)** dry deposition and **(b)** wet deposition fields at 11 October 2001, 21:00 UTC.

[Title Page](#)[Abstract](#)[Introduction](#)[Conclusions](#)[References](#)[Tables](#)[Figures](#)[◀](#)[▶](#)[◀](#)[▶](#)[Back](#)[Close](#)[Full Screen / Esc](#)[Print Version](#)[Interactive Discussion](#)

© EGU 2003

Methodology for  
prediction of risk

A. Baklanov et al.

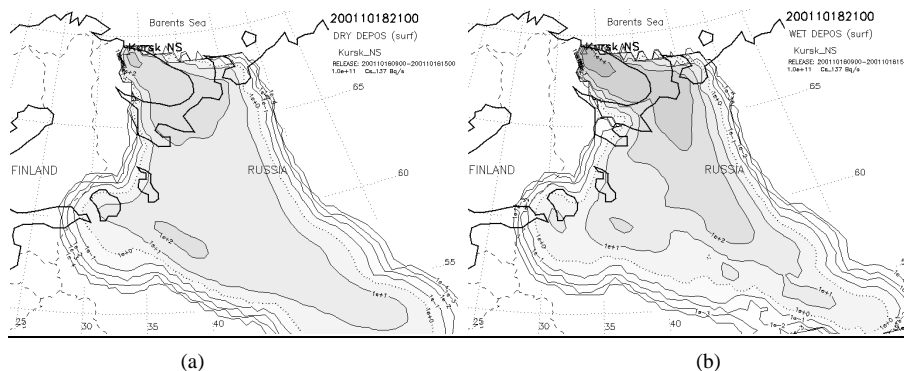


**Fig. 9.** Specific case of 16 October 2001 for the “unit discrete hypothetical release” of  $^{137}\text{Cs}$  at the Roslyakovo shipyard: **(a)** dry deposition and **(b)** wet deposition fields at 18 October 2001, 21:00 UTC.

Title Page

Abstract

Introduction

Conclusions

References

Tables

Figures

◀

▶

◀

▶

Back

Close

Full Screen / Esc

Print Version

Interactive Discussion

© EGU 2003

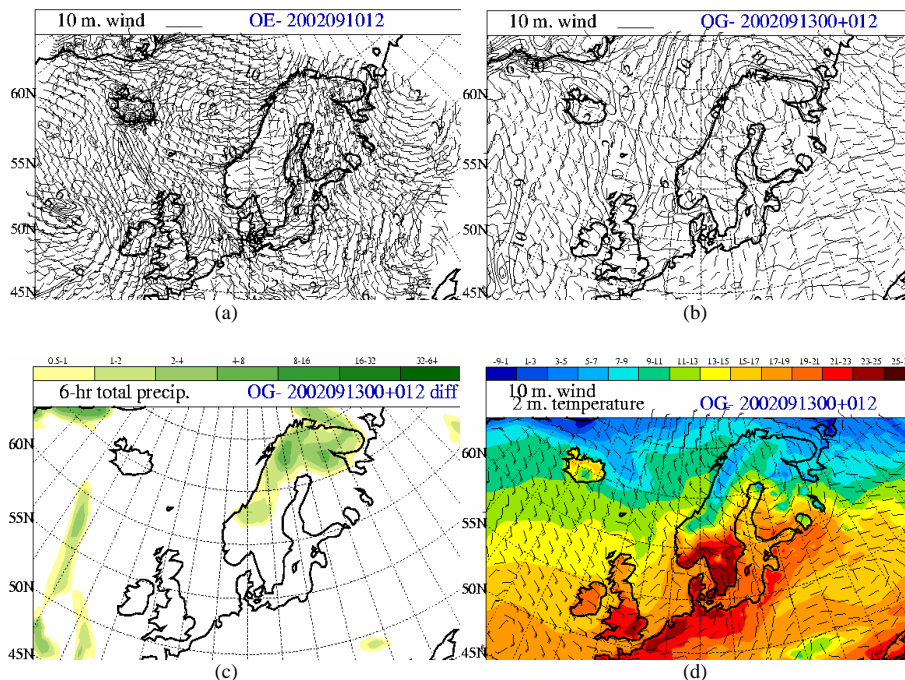


**Fig. 10.** Specific case of 10 September 2002 – meteorological fields: **(a)** analysed wind at 10 m for 10 September 2002, 12:00 UTC (DMI-HIRLAM, E-version), **(b)** forecasted wind at 10 m for 13 September 2002, 12:00 UTC (DMI-HIRLAM, G-version), **(c)** forecasted 6-hour precipitation for 13 September 2002, 12:00 UTC, and **(d)** forecasted wind at 10 m and temperature at 2 m for 13 September 2002, 12:00 UTC.

[Title Page](#)
[Abstract](#)
[Introduction](#)
[Conclusions](#)
[References](#)
[Tables](#)
[Figures](#)
[◀](#)
[▶](#)
[◀](#)
[▶](#)
[Back](#)
[Close](#)
[Full Screen / Esc](#)
[Print Version](#)
[Interactive Discussion](#)



Methodology for  
prediction of risk

A. Baklanov et al.

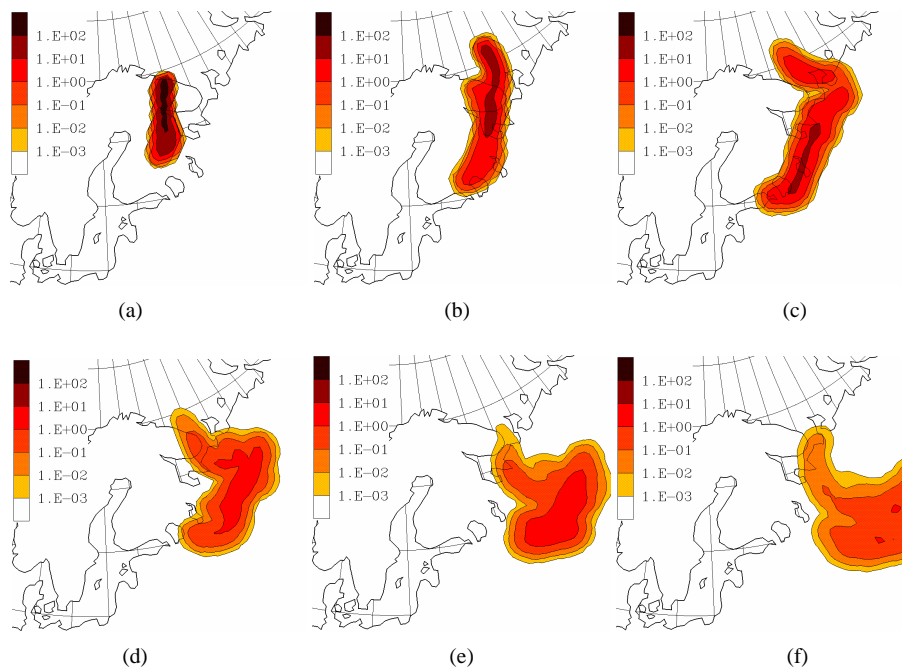


**Fig. 11.** Specific case of 10 September 2002 for the “unit discrete hypothetical release” of  $^{137}\text{Cs}$  at the Snezhnogorsk shipyard (Nerpa): surface air concentration fields at: **(a)** 11 September 2002, 00:00 UTC, **(b)** 11 September 2002, 12:00 UTC, **(c)** 12 September 2002, 00:00 UTC, **(d)** 12 September 2002, 12:00 UTC, **(e)** 13 September 2002, 00:00 UTC, and **(f)** 13 September 2002, 12:00 UTC.

[Title Page](#)[Abstract](#)[Introduction](#)[Conclusions](#)[References](#)[Tables](#)[Figures](#)[◀](#)[▶](#)[◀](#)[▶](#)[Back](#)[Close](#)[Full Screen / Esc](#)[Print Version](#)[Interactive Discussion](#)

© EGU 2003

Methodology for  
prediction of risk

A. Baklanov et al.

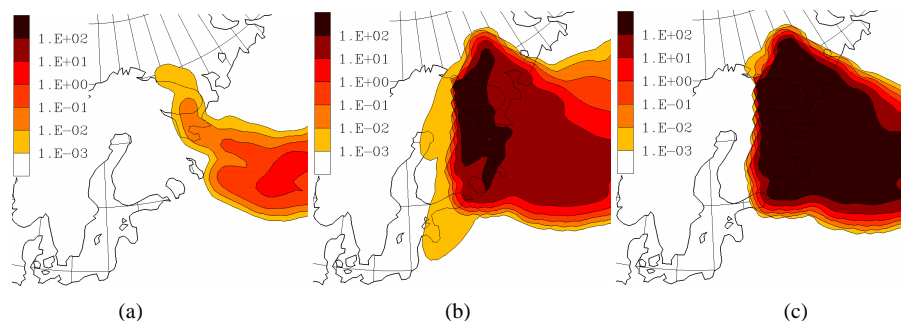


**Fig. 12.** Specific case of 10 September 2002 for the “unit discrete hypothetical release” of  $^{137}\text{Cs}$  at the Snezhnogorsk shipyard: **(a)** surface air concentration field at 14 September 2002, 00:00 UTC; **(b)** integrated in time air concentration in the surface layer field at 15 September 2002, 18:00 UTC, and **(c)** total deposition field at 14 September 2002, 00:00 UTC.

[Title Page](#)[Abstract](#)[Introduction](#)[Conclusions](#)[References](#)[Tables](#)[Figures](#)[◀](#)[▶](#)[◀](#)[▶](#)[Back](#)[Close](#)[Full Screen / Esc](#)[Print Version](#)[Interactive Discussion](#)

© EGU 2003